Correlation of the structural and functional domains in the membrane protein Vpu from HIV-1

F. M. Marassi*†, C. Ma*, H. Gratkowski*, S. K. Straus*, K. Strebel‡, M. Oblatt-Montal§, M. Montal§, and S. J. Opella*¶

*Department of Chemistry, University of Pennsylvania, Philadelphia, PA 19104; †Wistar Institute, Philadelphia, PA 19104; ‡Laboratory of Molecular Microbiology, National Institute of Allergy and Infectious Diseases, National Institutes of Health, Bethesda, MD 20892; and §Department of Biology, University of California, San Diego, La Jolla, CA 92093

Vpu is an 81-residue membrane protein encoded by the HIV-1 genome. NMR experiments show that the protein folds into two distinct domains, a transmembrane hydrophobic helix and a cytoplasmic domain with two in-plane amphipathic α-helices separated by a linker region. Resonances in one-dimensional solid-state NMR spectra of uniformly ^{15}N labeled Vpu are clearly segregated into two bands at chemical shift frequencies associated with NH bonds in a transmembrane α-helix, perpendicular to the membrane surface, and with NH bonds in the cytoplasmic helices parallel to the membrane surface. Solid-state NMR spectra of truncated Vpu_{2-51} (residues 2–51), which contains the transmembrane α-helix and the first amphipathic helix of the cytoplasmic domain, and of a construct Vpu_{28-81} (residues 28–81), which contains only the cytoplasmic domain, support this structural model of Vpu in the membrane. Full-length Vpu (residues 2–81) forms discrete ion-conducting channels of heterogeneous conductance in lipid bilayers. The most frequent conductances were 22 ± 3 pS and 12 ± 3 pS in 0.5 M KCl and 29 ± 3 pS and 12 ± 3 pS in 0.5 M NaCl. In agreement with the structural model, truncated Vpu_{2-51}, which has the transmembrane helix, forms discrete channels in lipid bilayers, whereas the cytoplasmic domain Vpu_{28-81}, which lacks the transmembrane helix, does not. This finding shows that the channel activity is associated with the transmembrane helical domain. The pattern of channel activity is characteristic of the self-assembly of conductive oligomers in the membrane and is compatible with the structural and functional findings.

The lifecycle of HIV-1, the retrovirus that causes AIDS, is intimately associated with membranes. Infection starts with the viral envelope recognizing and fusing with susceptible cells and ends with the budding of new virus particles from the membranes of infected cells. Thus, membrane proteins are responsible for many functions essential for the propagation and virulence of HIV-1 infections.

Vpu, one of four accessory proteins encoded in the HIV-1 genome, is an 81-residue membrane protein (1–3). A growing body of evidence from biological, functional, and structural studies indicates that its two principal biological activities are associated with different structural domains of the protein (4). Vpu facilitates the budding of new virus particles from infected cells (1, 5); without active protein, newly formed virions accumulate in the cells resulting in increased cytotoxicity (6). The oligomerization of the transmembrane helical domain of Vpu in membranes, which results in ion-channel activity (7, 8) and may influence the budding process (9), has been analyzed with molecular simulations and modeling (10, 11). Oligomerization resulting in ion-channel activity is in keeping with the sequence similarity between Vpu and the influenza virus M2 ion-channel protein (8, 12). Vpu also enhances the degradation of CD4 (13), an activity associated with interactions between the cytoplasmic domains of Vpu and CD4 (14–16). In the absence of Vpu, processing of gp160 to form the gp41 and gp120 polypeptides is impaired because of the formation of stable complexes with CD4 in the endoplasmic reticulum (ER) of infected cells (13). Thus, Vpu indirectly regulates processing of gp160 in the trans-Golgi compartment into the gp120 and gp41 proteins needed for the assembly of infectious virus particles (17).

Vpu is an ideal target for the emerging NMR approaches to structure determination of membrane proteins in lipid environments (18, 19). Solid-state NMR experiments on oriented samples enable the three-dimensional structures of membrane proteins to be determined in the definitive environment of fully hydrated phospholipid bilayers (20, 21). The three-dimensional structures of a channel-forming polypeptide corresponding to the M2 segment of the nicotinic acetylcholine receptor (22) and of the gramicidin ion-channel peptide (23) were determined recently with this approach. Complete structure determination requires the resolution and assignment of all resonances of uniformly labeled samples with multidimensional solid-state NMR experiments (24–26). However, the initial one- and two-dimensional solid-state NMR spectra of oriented samples provide valuable information about the architecture of helical proteins associated with membrane bilayers. This strategy was shown to work with the influenza virus M2 (27), colicin E1 (28, 29), and other membrane-associated polypeptides (29), because of the well characterized angular dependence of the ^{15}N amide chemical shift and ^1H–^{15}N heteronuclear dipolar spin interactions.

Herein, we describe the topology, structural features, and channel activity of full-length Vpu and its individual domains, based on solution NMR experiments of phospholipid micelle samples, solid-state NMR experiments on oriented phospholipid bilayer samples, and measurements of channel recordings in phospholipid bilayers. Vpu folds into two distinct domains. Both of the amphipathic helices in the cytoplasmic domain lie in the plane of the bilayer; in contrast, the transmembrane hydrophobic helix is perpendicular to the plane of the bilayer. The structural properties of these domains are strongly correlated with the ion-channel activity measured after reconstitution in lipid bilayers. Oligomerization of the transmembrane helices results in the formation of a functional ion-conductive channel.

Materials and Methods

Protein Expression and Purification. The *vpu* gene from the HIV-1 isolate HTLVIII_B (30) was cloned into the expression vector pMMHa (31). The detailed procedure for the cloning, expression, and purification, as well as the biological activities of full-length Vpu and the truncated constructs will be published elsewhere. Briefly, *Escherichia coli* strain BL21 (DE3) cells were transformed with the plasmid vectors carrying the target constructs and grown in minimal medium containing 100 μg/ml ampicillin, 7.0 g/liter Na_2HPO_4, 3.0 g/liter KH_2PO_4, 0.5 g/liter NaCl, 0.1 mM $CaCl_2$, 1 mM $MgSO_4$, 50 mg/liter thiamine, 1%

(vol/vol) LB broth, 10 g/liter D-glucose, and 1 g/liter $(NH_4)_2SO_4$. For uniformly ^{15}N-labeled proteins, $(^{15}NH_4)_2SO_4$ (Cambridge Isotope Laboratories, Andover, MA) was supplied as the sole nitrogen source.

The cells were lysed by resuspending in 50 mM Tris-Cl, pH 8.0/15% (vol/vol) glycerol/1 mM NaN$_3$/50 μg/ml lysozyme (Roche Molecular Biochemicals). The cell lysate was sonicated (duty cycle 30%, output control 5, Branson Sonifier 450, micro tip) and then centrifuged at 35,000 × g for 30 min. The supernatant was discarded, and the pellet was sonicated in 50 mM Tris-Cl, pH 8.0/1% (wt/vol) deoxycholic acid/1% (vol/vol) IGEPAL CA-630 (Sigma)/1 mM NaN$_3$ and then centrifuged at 35,000 × g for 30 min. The resulting pellet was sonicated twice for 4 min on ice in binding buffer (6 M guanidine hydrochloride/5 mM imidazole/0.5 M NaCl/20 mM Tris-Cl, pH 8.0). After 10-fold dilution with water, precipitation of inclusion bodies was observed. The precipitate was collected by centrifugation at 28,000 × g for 1 h, and the resulting pellet was dissolved in binding buffer and stored at 4°C overnight. Nickel affinity chromatography (His·Bind Resin, Novagen) enabled the separation of the His-tagged fusion protein from other proteins in the inclusion bodies.

Cyanogen bromide was used to cleave Vpu from the fusion partner (32). The two Met residues in the Vpu sequence have been changed to Leu to facilitate cyanogen bromide cleavage of the fusion protein systems used for expression and purification. The sequence of cleaved, recombinant full-length Vpu polypeptide is QPIQIAIVAL VVAIIIAIVV WSIVIIEYRK ILRQRKIDRL IDRLIERAED SGNESEGEIS ALVELGVELG HHAPWDVDDL.

Recombinant Vpu and Vpu$_{2-51}$ were purified by means of preparative reverse-phase HPLC on a Delta-Pak C4 column (15 μM, 300 Å, 7.8 × 300 mm, Waters) with a water-acetonitrile gradient. For the isolation of Vpu$_{28-81}$, the lyophilized cleavage mixture was dissolved in 8 M urea/20 mM Tris-Cl, pH 8.0/50 mM NaCl/1 mM NaN$_3$ buffer and then loaded on to a Q Sepharose Fast Flow column (Amersham Pharmacia). Vpu$_{28-81}$ was eluted in the same buffer with 500 mM NaCl. The Vpu$_{28-81}$ fraction was concentrated (5 mg/ml) and purified by gel filtration FPLC on a Superdex 75 HR 10/30 column (Amersham Pharmacia) in 8 M urea/20 mM Tris-Cl, pH 8.0/200 mM NaCl/1 mM NaN$_3$ with a flow rate of 0.7 ml/min. Vpu$_{28-81}$ was purified further by using HPLC with a Delta-Pak C18 column (15 μM, 300 Å, 7.8 × 300 mm, Waters).

Solution NMR Spectroscopy. Solution NMR samples were prepared by mixing an appropriate amount of labeled protein with 270 μl of micellar solution containing 200 mM d$_{40}$-dihexanoyl phosphatidylcholine (Cambridge Isotope Laboratories), 10% (vol/vol) ^2H_2O, and 5 mM NaN$_3$ at pH 4.0. The samples were centrifuged at 12,000 × g for 5 min, and the supernatants were transferred to 5-mm Shigemi NMR tubes (Shigemi, Allison Park, PA). The sample tubes were placed in triple-resonance 5-mm probes with three-axis field gradients. The solution NMR experiments were performed on Bruker (Billerica, MA) DMX 600 or DMX 750 spectrometers. The two-dimensional heteronuclear single quantum correlation (33) spectra were obtained on samples with a protein concentration of 0.4 mM at 50°C. The ^{15}N and ^1H chemical shifts were referenced to 0 ppm for liquid ammonia and tetramethylsilane, respectively. The NMR data were processed by using the program FELIX (M.S.I., San Diego) on a S.G.I. computer workstation (Mountain View, CA).

Solid-State NMR Spectroscopy. For Vpu and Vpu$_{2-51}$ containing the hydrophobic transmembrane helix, 2 mg of protein were dissolved in 0.5 ml of 500 mM SDS water solution. Unilamellar vesicles were prepared by sonication of 100 mg of 4:1 dioleoyl phosphatidylcholine:dioleoyl phosphatidylglycerol (Avanti Bio-

chemicals, Alabaster, AL) in water by using a Branson sonifier equipped with a micro tip. The protein solution was mixed with the vesicles, and this mixture was diluted by the addition of 30 ml of water, quickly frozen in liquid nitrogen and allowed to thaw at 22°C. SDS was removed by dialysis against three 4-liter changes of 10 mM Tris-Cl (pH 7.4), followed by three 4-liter changes of water. For Vpu$_{28-81}$ containing only the cytoplasmic domain, 4 mg of protein were dissolved in water. This solution was added directly to the vesicle preparation, and the mixture was frozen and thawed three times. Planar lipid bilayers oriented on glass slides were prepared from the reconstituted vesicles as described (24). The samples were sealed in a polymer wrap before insertion in the radio frequency coil of the NMR probe.

The solid-state NMR spectra were obtained at 0°C by using home-built double-resonance probes with "square" radio frequency coils wrapped directly around the samples. The spectrometers had magnets with field strengths corresponding to ^1H resonance frequencies of 700 MHz and 400 MHz. Conditions for the one-dimensional cross-polarization (34, 35) and the two- and three-dimensional polarization inversion spin exchange at the magic angle (PISEMA; refs. 36 and 37) solid-state NMR experiments were as described (24). The ^{15}N and ^1H chemical shifts were referenced to 0 ppm for liquid ammonia and tetramethylsilane, respectively. The NMR data were processed by using the program FELIX on a Silicon Graphics computer workstation.

Single-Channel Recordings in Planar Lipid Bilayers. Lipid bilayers were assembled by apposition of two monolayers spread from a lipid solution in hexane as described (8, 22). The lipids were diphytanoyl phosphatidylethanolamine and diphytanoyl phosphatidylcholine (Avanti Biochemicals) at a 4:1 ratio in hexane (5 mg/ml). The aqueous subphase was composed of 0.5 M KCl or 0.5 M NaCl, and 5 mM Hepes (pH 7.4). Purified recombinant polypeptides were dissolved in trifluoroethanol at 0.01 mg/ml and added to the aqueous subphase after bilayer formation. Single-channel currents were recorded between the range −100 mV ≤ V ≤ 100 mV. Acquisition and analysis of single-channel currents were performed as described (8, 22). Records were filtered at 1 kHz with an 8-pole Bessel filter (Frequency Devices, Haverhill, MA) and digitized at 0.1 ms per point by using an Axon TL-1 interface (Axon Instruments, Foster City, CA). Data processing was performed with a pClamp 5.5 (Axon Instruments). The illustrated channel recordings are representative of the most frequently observed conductances under the specified experimental conditions. Single-channel conductance was calculated from Gaussian fits to current histograms, and the channel open and closed lifetimes were calculated from exponential fits to probability density functions by using data from segments of continuous recordings lasting longer than 30 s and with 300 events (means ± SEM). Openings shorter than 0.3 ms were ignored. Bilayer reconstitution experiments were performed at 24 ± 2°C.

Calculation of Solid-State NMR Spectra. Two-dimensional PISEMA spectra were calculated on a Silicon Graphics O2 computer by using the FORTRAN program FINGERPRINT, developed in our laboratory. FINGERPRINT is based on previously described methods (38, 39). The spectral frequencies (^{15}N chemical shift and ^1H–^{15}N dipolar coupling) were calculated for various orientations of a 17-residue α-helix, with 3.6 residues per turn, and uniform backbone dihedral angles for all residues ($\psi = -57°$; $\phi = -47°$). The specified helix orientation, the backbone dihedral angles, the ^{15}N chemical shift tensor, and the NH bond distance were input to FINGERPRINT. The principal values and molecular orientation of the ^{15}N chemical shift tensor ($\sigma_{11} = 64$ ppm; $\sigma_{22} = 77$ ppm; $\sigma_{33} = 217$ ppm; σ_{11} 208 NH = 17°), and the NH bond distance (1.07Å) were as previously determined (40). For each helix orientation, the backbone atomic coordinates

were calculated by using the FORTRAN program COORDINATE, also developed in our lab. The helices were visualized with the program RASMOL (klaatu.oit.umass.edu/microbio/rasmol/).

Results

Domains of Vpu. Hydropathy (41) and density alignment surface (42) analyses predict that the N-terminal domain of full-length Vpu is α-helical. Experimental solid-state NMR measurements show (29) that full-length Vpu has a single N-terminal transmembrane helix. Previous solution NMR studies of synthetic and recombinant polypeptides corresponding to the cytoplasmic domain of Vpu have given conflicting results, most likely because combinations of solvents and salts rather than lipids were used to solubilize the samples (43–45). Three-dimensional triple-resonance solution NMR experiments on uniformly ^{2}H-/^{13}C-/^{15}N-labeled samples in dihexanoyl phosphatidylcholine micelles enabled us to make complete backbone resonance assignments and to determine the secondary structure of the cytoplasmic domain of recombinant Vpu$_{28-81}$ (residues 28–81). In lipid environments, the cytoplasmic domain of Vpu has two distinct α-helices separated by a linker region that contains the two highly conserved Ser residues (positions 52 and 56), which can be phosphorylated (44).

In addition to the cytoplasmic domain, we have expressed a number of other constructs of Vpu, including polypeptides corresponding to full-length Vpu (residues 2–81) and a truncated form, Vpu$_{2-51}$ (residues 2–51), containing only the transmembrane hydrophobic helix and the first amphipathic helix of the cytoplasmic domain. The expressed polypeptides were used in three types of experiments: solution NMR on phospholipid micelles, solid-state NMR on oriented phospholipid bilayers, and channel recordings on phospholipid bilayers. The results from these experiments enable the direct correlation of structure, topology, and function of this membrane protein.

Solution NMR Spectroscopy. The two-dimensional heteronuclear single quantum correlation NMR spectra of all three polypeptides in dihexanoyl phosphatidylcholine micelles are notable, because the correlation resonances from backbone amide sites that are present have essentially identical ^{1}H and ^{15}N chemical shift frequencies (Fig. 1 A–C). This pattern holds true for resonances assigned to residues in the transmembrane helix and the cytoplasmic domain. For example, the resonances assigned to Gly-53, Gly-58, Gly-67, and Gly-71 in the cytoplasmic domain have the same resonance frequencies in the spectra from Vpu and Vpu$_{28-81}$ (red boxes) and are absent, as expected, from the spectrum from Vpu$_{2-51}$ (Fig. 1B). Likewise, for Trp-22 in the transmembrane helix and Trp-76 in the second cytoplasmic helix, their respective indole resonances have identical chemical shift frequencies in the spectra of the two constructs (red/blue boxes). The resonance from Ser-23 in the transmembrane helix has the same chemical shift frequencies in the spectra of the two constructs containing the transmembrane helix, Vpu and Vpu$_{2-51}$ (blue boxes), and is not present in the spectrum of the cytoplasmic domain Vpu$_{28-81}$ (Fig. 1C). These results indicate that the transmembrane and cytoplasmic domains of Vpu fold independently in membrane environments, adopt the same three-dimensional structures regardless of which other segments are present, and do not interact strongly with each other.

Solid-State NMR Spectroscopy. The one-dimensional solid-state ^{15}N NMR spectra in Fig. 1 D–F were used to determine the orientations of the three helical segments of Vpu in the membrane, as illustrated with the drawings in Fig. 1. The resonances in the solid-state NMR spectrum of full-length Vpu (Fig. 1D) are clearly segregated into two distinct bands at chemical shift frequencies associated with NH bonds in the transmembrane helix perpendicular to the membrane surface (200 ppm) and with
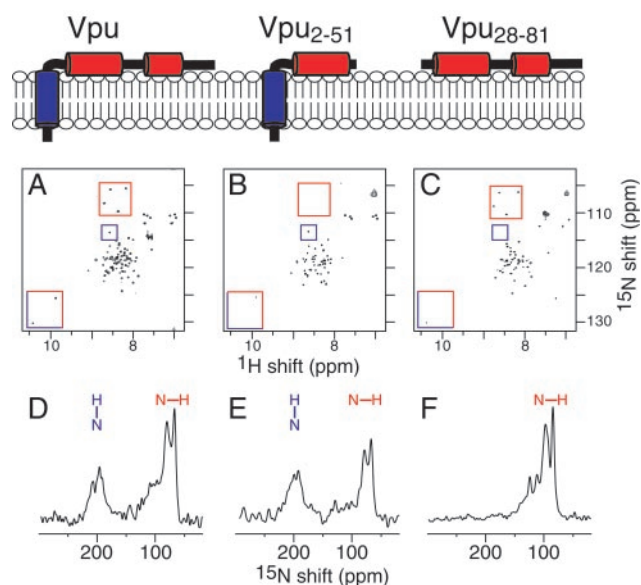

Fig. 1. NMR spectra of three uniformly ^{15}N-labeled recombinant Vpu constructs. Vpu has three helical segments. (*Top*) The overall architecture of the three constructs used in this study in the context of a membrane bilayer, with the hydrophobic helix in blue and both amphipathic helices in red. (*Middle*) Two-dimensional heteronuclear single quantum correlation spectra of the three Vpu constructs in dihexanoyl phosphatidylcholine micelles: Vpu (*A*), Vpu$_{2-51}$ (*B*), and Vpu$_{28-81}$ (*C*). Representative assigned resonances are highlighted in the boxes: amide resonances from Gly-53, Gly-58, Gly-67, and Gly-71 (red boxes); Ser-23 (blue boxes); and indole resonances from Trp-22 and Trp-76 (red/blue boxes). (*Bottom*) One-dimensional solid-state ^{15}N NMR spectra of the three Vpu constructs obtained at 0°C in oriented lipid bilayers: Vpu (*D*), Vpu$_{2-51}$ (*E*), and Vpu$_{28-81}$ (*F*). The orientations of transmembrane (blue) and in-plane (red) amide NH bonds are indicated above the spectra.

NH bonds in both cytoplasmic helices parallel to the membrane surface (70 ppm). The spectra of Vpu$_{2-51}$ and Vpu$_{28-81}$ strongly support the models shown in Fig. 1. The cytoplasmic domain, which is soluble but unfolded and highly flexible in water, adopts a unique conformation in the presence of phospholipids and binds strongly to the membrane surface in a unique orientation. The three solid-state NMR spectra have nearly identical features in the spectral regions associated with both transmembrane and in-plane helices. Vpu has structural features typical of those found in other small membrane proteins. Indeed, the structure of the 50-residue Vpu$_{2-51}$ polypeptide is very similar to the structures previously determined by using this NMR approach for the 46-residue Pf1 coat protein (46) and the 50-residue fd coat protein in membrane environments (47).

These findings are refined and confirmed with multidimensional solid-state NMR spectra. Two-dimensional PISEMA (^{1}H–^{15}N dipolar coupling/^{15}N chemical shift) spectral planes from uniformly ^{15}N-labeled full-length Vpu in an oriented bilayer sample are presented in Fig. 2. In the complete two-dimensional PISEMA spectrum (Fig. 2B), each amide site in the protein contributes a single correlation peak characterized by unique ^{1}H–^{15}N dipolar coupling and ^{15}N chemical shift frequencies. Approximately 16 resonances can be discerned in the spectral region (8-kHz dipolar coupling and 200-ppm chemical shift) associated with a transmembrane helix. The "wheel-like" pattern of resonances observed in this region of the spectrum is characteristic of a tilted transmembrane α-helix and provides an index of the slant and polarity of the helix, as well as the overall topology of Vpu in the membrane. This analysis shows that full-length Vpu has a single transmembrane helix. It is the resolution of 15–16 resonances in this spectral region for each
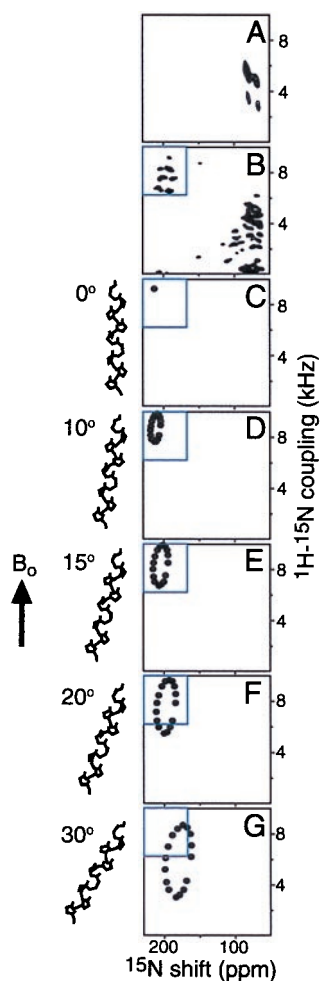
Fig. 2. Two-dimensional solid-state NMR ^{1}H–^{15}N dipolar coupling/^{15}N chemical shift correlation PISEMA planes from uniformly ^{15}N-labeled full-length Vpu in oriented lipid bilayers. (*A*) Plane extracted from a three-dimensional ^{1}H chemical shift/^{15}N dipolar coupling/^{15}N chemical shift spectrum at the ^{1}H chemical shift frequency of 15.9 ppm. (*B*) Two-dimensional PISEMA spectrum. (*C–G*) Two-dimensional PISEMA spectra calculated for a 17-residue α-helix, with uniform dihedral angles ($\phi = -57°$; $\psi = -47°$) for the transmembrane orientations 0° (*C*), 10° (*D*), 15° (*E*), 20° (*F*), and 30° (*G*) between the long axis of the transmembrane helix and the normal to the membrane plane. The blue box highlights the spectral region occupied by resonances in the two-dimensional PISEMA spectrum from residues in the single transmembrane helix of Vpu.

transmembrane helix present in the protein that provides the definitive evidence of the topology in the membrane, as has been shown with fd coat protein (24), M2 channel peptide (22), and colicin E1 polypeptide (28). There is substantial overlap among the resonances from the cytoplasmic domain of the protein (0–5 kHz and 70–90 ppm) because of the similar in-plane orientations of the helices. Spectral resolution in this region is possible with three-dimensional correlation spectroscopy (37, 48). The third spectral dimension is the ^{1}H chemical shift, and a plane extracted from a three-dimensional data set at the ^{1}H chemical shift frequency of 15.9 ppm is presented in Fig. 2*A*. Several individual resonances from amide sites in the cytoplasmic domain can be observed.

It is possible to calculate solid-state NMR spectra for specific models of proteins in oriented samples, because the frequencies reflect the angles between individual bonds or chemical groups and the direction of the applied magnetic field. Spectra calcu-

lated for several orientations of a 17-residue transmembrane α-helix, with 3.6 residues per turn, and identical backbone dihedral angles for all residues ($\psi = -57°$; $\phi = -47°$), are shown in Fig. 2 *C–G*. The spectral frequencies reflect the helix orientation and backbone dihedral angles, as well as the ^{15}N amide chemical shift tensor and the NH bond length. Variations in the backbone dihedral angles of ±10° can lead to differences as large as ±15 ppm of the ^{15}N chemical shift frequencies but only ±1 kHz of the ^{1}H–^{15}N dipolar coupling frequencies. Variations in the magnitudes of the principal elements of the ^{15}N chemical shift tensors of ±20 ppm can lead to differences as large as ±15 ppm in the calculated ^{15}N chemical shift frequencies. Such residue-dependent variability is observed for the magnitudes of the principal elements of the amide ^{15}N chemical shift tensor; in contrast, little variability has been observed in the tensor orientations (49). Finally, variations in the NH bond length as large as ±0.02 Å can result in changes as large as ±0.6 kHz in the calculated ^{1}H–^{15}N dipolar coupling frequency. These considerations make the ^{1}H–^{15}N dipolar coupling the more reliable spectral parameter for estimating the tilt of a transmembrane helix in the bilayer. Based on the comparisons of the calculated spectra with the experimental spectrum in Fig. 2, the transmembrane helix of Vpu has a tilt of approximately 15° from the bilayer normal. A single resonance assignment would suffice to determine the polarity of the Vpu α-helix in the membrane. Of course, only the sequential assignment of all of the resonances and the calculation of the three-dimensional structure can provide the definitive answer about the tilt of the helix in the bilayer (22).

Channel Measurements. Vpu forms discrete ion-conductive channels of heterogeneous conductance in lipid bilayers. At pH 7.4, the most frequent channels detected have a conductance of 22 ± 3 pS (Fig. 3*A*) and 29 ± 3 pS (Fig. 3*B*) in 0.5 M KCl and 0.5 M NaCl, respectively. In addition to the primary conductances, a second discrete channel conductance of 12 ± 3 pS occurred at high frequency (Fig. 3*A*). Smaller and larger channel conductances were also detected with progressively lower occurrence. This pattern of channel activity is characteristic of amphipathic ion-channel-forming peptides and proteins and presumably results from the self-assembly of noncovalently bonded oligomers, the conductance of which increases with the number of subunits (8, 22). The most frequent conductance observed for full-length Vpu (22 pS in KCl and 29 pS in NaCl) is compatible with a structure consisting of a water-filled five-helix bundle arising from the self-assembly of Vpu monomers.

There is a strong correlation between the structural features of the three polypeptides and their ion-channel activity determined after reconstitution in lipid bilayers. This correlation is illustrated with the channel recordings and analysis in Fig. 3. The two polypeptides containing the transmembrane α-helix, full-length Vpu, and Vpu$_{2–51}$ have ion-channel activity. In contrast, the cytoplasmic domain construct Vpu$_{28–81}$ without the transmembrane helix has no recognizable ion-channel activity. Only irregular stray current fluctuations were detected, indicating that Vpu$_{28–81}$ interacts with membranes in a nonspecific manner. These results show that the ion-channel activity of Vpu is confined to the transmembrane domain in expressed polypeptides and are consistent with an earlier study that used synthetic peptides (8).

Discussion

The genome of HIV is only about 10 kilobases and encodes all the proteins necessary to enter, replicate within, and bud from susceptible helper T cells. This minimal set of proteins must therefore provide the essential components to complete the life cycle of HIV efficiently within cells. Vpu is unique to HIV-1 and is one of four accessory or regulatory proteins encoded by the HIV genome. A hallmark of AIDS progression is the gradual
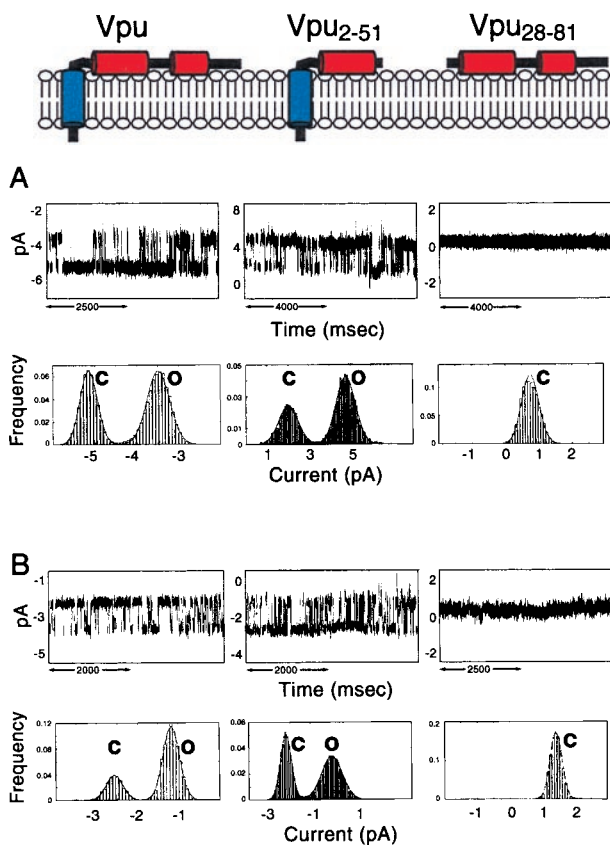
Fig. 3. Single-channel recordings from three Vpu constructs: Vpu (*Left*), Vpu$_{2-51}$ (*Center*), and Vpu$_{28-81}$ (*Right*) in symmetric 0.5 M KCl (*A*) or 0.5 M NaCl (*B*) and 10 mM Hepes (pH 7.4). Short segments of continuous recordings were selected to illustrate the occurrence of the 22-pS (K$^+$) and 29-pS (Na$^+$) channel for full-length Vpu and the 26-pS (K$^+$) and 23-pS (Na$^+$) channel for truncated Vpu$_{2-51}$. The cytoplasmic domain Vpu$_{28-81}$ does not form ion channels. Note the occurrence of only stray, erratic fluctuations in membrane current produced by Vpu$_{28-81}$ in contrast with the square events produced by Vpu and Vpu$_{2-51}$. The currents of the closed (C) and open (O) states are indicated. Upward deflection indicates channel opening. Corresponding cumulative current histograms and Gaussian fits for the primary conductances generated from continuous segments of recordings lasting several minutes. (*A*) For Vpu, the probability of the channel being open (P_o) is 0.56 recorded at 85 mV. For Vpu$_{2-51}$, $P_o = 0.76$ recorded at 100 mV. (*B*) For Vpu, $P_o = 0.75$ recorded at 50 mV; for Vpu$_{2-51}$, $P_o = 0.56$ recorded at 50 mV.

depletion of CD4$^+$ helper T cells. This depletion is, at least in part, the consequence of a rapid down-modulation of CD4 after HIV infection and involves the activities of Env, Nef, as well as Vpu (for a review see ref. 50). Each of these proteins acts through a different mechanism: Env and Vpu prevent transport of *de novo* synthesized CD4 to the cell-surface through the formation of stable complexes in the ER and the targeting of CD4 to the ubiquitin-dependent proteasome pathway, respectively; Nef, in contrast, induces down-modulation of preexisting CD4 from the cell surface with subsequent degradation in the

lysosomes. Aside from its involvement in CD4 down-modulation, Vpu is also essential for the budding of new virions from infected cells. These two biological activities of Vpu have been correlated with two distinct structural domains in the Vpu protein, an N-terminal transmembrane helix and a C-terminal cytoplasmic domain. There is compelling evidence implicating the cytoplasmic domain of Vpu in CD4 degradation. In the ER, Vpu binds to CD4 and targets it for proteolysis in the cytosolic ubiquitin-proteasome pathway. Vpu mediates this process by binding to β-TrCP (β-transducin repeats containing protein), which in turn binds to the proteasome-targeting factor Skp1p (14). Indeed, a ternary complex consisting of CD4–Vpu–β-TrCP has been identified, and binding of Vpu to β-TrCP requires the two phosphoserine residues 52 and 56 that are essential for CD4 degradation (14). The integrity of the transmembrane domain is required for virion release.

The molecular mechanism by which the Vpu transmembrane domain facilitates the budding of new viral particles is not clear. Nonetheless, oligomerization of the transmembrane domain has been shown to result in the formation of ion channels (7, 8, 15). Several models may be envisioned for the role of a Vpu channel in the budding process. At the ER, oligomerization of Vpu could induce the formation of channels and could result in the collapse of the transmembrane potential across the ER cisternae and the acceleration of membrane fusion and protein traffic in the exocytic pathway. Alternatively, at the ER/mitochondrial junctions, Vpu may contribute to the collapse of the mitochondrial membrane potential and thereby promote apoptosis or compromise the energetic homeostasis of the cell. Finally, at the plasma membrane, insertion of Vpu channels may attenuate the cell resting potential and thereby promote fusion and release of new virions. These models are testable.

Our findings clearly show that Vpu folds into two distinct domains: a transmembrane N-terminal hydrophobic helix and a cytoplasmic domain that contains two amphipathic in-plane helices. Further, the structural motifs are highly correlated with specific functions. The ion-channel activity thought to be associated with the ability of Vpu to facilitate the budding of new virus particles is likely to result from the oligomerization of the transmembrane helix to form a water-filled helical bundle (8, 11, 15). The cytoplasmic domain is associated with the ability of Vpu to affect the CD4/gp160 complex on the cell surface. The crucial biological functions of HIV-1 accessory proteins affect the virulence of the infections. In the case of Vpu, the clear correlation of structure and function provides a first step toward the design of antiviral drugs (51).

1. Strebel, K., Klimkait, T. & Martin, M. A. (1988) *Science* **241,** 1221–1223.
2. Cohen, E., Terwilliger, E. F., Sordroski, J. G. & Haseltine, W. A. (1988) *Nature (London)* **334,** 532–534.
3. Matsuda, Z., Chou, M. J., Matsuda, M., Huang, J. H., Chen, Y. M., Redfield, R., Mayer, K., Essex, M. & Lee, T. H. (1988) *Proc. Natl. Acad. Sci. USA* **85,** 6968–6972.
4. Strebel, K. (1996) in *Human Retroviruses and AIDS 1996: A Compilation and Analysis of Nucleic Acid and Amino Acid Sequences*, eds. Myers, G., Korber, B. T., Foley, B. T., Jeang, K.-T., Mellors, J. W. & Wain-Hobson, S. (Los Alamos Natl. Lab., Los Alamos, NM), pp. 19–27.
5. Terwilliger, E. F., Cohen, E. A., Lu, Y., Sodroski, J. G. & Haseltine, W. A. (1989) *Proc. Natl. Acad. Sci USA* **86,** 5163–5167.
6. Klimkait, T., Strebel, K., Hoggan, M. D., Marin, M. A. & Orenstein, J. M. (1990) *J. Virol.* **64,** 621–629.
7. Ewart, G. D., Sutherland, T., Gage, P. W. & Cox, G. B. (1996) *J. Virol.* **70,** 7108–7115.
8. Schubert, U., Ferrer-Montiel, A. V., Oblatt-Montal, M., Henklein, P., Strebel, K. & Montal, M. (1996) *FEBS Lett.* **398,** 12–18.
9. Maldarelli, F., Chen, M. Y., Willey, R. L. & Strebel, K. (1993) *J. Virol.* **67,** 5056–5061.

10. Grice, A. L., Kerr, I. D. & Sansom, M. S. P. (1997) *FEBS Lett.* **405,** 299–304.
11. Moore, P. B., Zhong, Q., Husslein, T. & Klein, M. L. (1998) *FEBS Lett.* **431,** 143–148.
12. Lamb, R. A. & Pinto, L. H. (1997) *Virology* **229,** 1–11.
13. Willey, R. L., Maldarelli, F., Martin, M. A. & Strebel, K. (1992) *J. Virol.* **66,** 7193–7200.
14. Bour, S., Schubert, U. & Strebel, K. (1995) *J. Virol.* **69,** 1510–1520.
15. Schubert, U., Bour, S., Ferrer-Montiel, A. V., Montal, M., Maldarelli, F. & Strebel, K. (1996) *J. Virol.* **70,** 809–819.
16. Margottin, F., Benichou, S., Durand, H., Richard, V., Liu, X., Gomas, E. & Benarous, R. (1996) *Virology* **223,** 381–386.
17. Margottin, F., Bour, S. P., Durand, H., Selig, G., Benichou, S., Richard, V., Thomas, O., Strebel, K. & Benarous, R. (1998) *Mol. Cell* **1,** 565–574.
18. Opella, S. (1997) *Nat. Struct. Biol.* **4,** 845–848.
19. Griffin, R. (1998) *Nat. Struct. Biol.* **5,** 508–512.
20. Cross, T. A. & Opella, S. J. (1994) *Curr. Opin. Struct. Biol.* **4,** 574–581.
21. Marassi, F. M. & Opella, S. J. (1998) *Curr. Opin. Struct. Biol.* **8,** 640–648.
22. Opella, S. J., Marassi, F. M., Gesell, J. J., Valente, A. P., Kim, Y., Oblatt-Montal, M. & Montal, M. (1999) *Nat. Struct. Biol.* **6,** 374–379.
23. Ketchem, R. R., Hu, W. & Cross, T. A. (1993) *Science* **261,** 1457–1460.
24. Marassi, F. M., Ramamoorthy, A. & Opella, S. J. (1997) *Proc. Natl. Acad. Sci. USA* **94,** 8551–8556.
25. Marassi, F. M., Gesell, J. J., Valente, A. P., Oblatt–Montal, M., Montal, M. & Opella, S. J. (1999) *J. Biomol. NMR* **14,** 141–148.
26. Tan, W. M., Gu, Z., Zeri, A. C. & Opella S. J. (1999) *J. Biomol. NMR* **13,** 337–342.
27. Kovacs, F. A. & Cross, T. A. (1997) *Biophys. J.* **73,** 2511–2517.
28. Kim, Y., Valentine, K., Opella, S. J., Schendel, S. L. & Cramer, W. A. (1998) *Protein Sci.* **7,** 342–348.
29. Marassi, F. M., Almeida, F. C. L., Kim, Y., Zasloff, M., Schendel, S. L., Cramer, W. A. & Opella, S. J. (1996) *Biophys. J.* **70,** A101 (abstr.).
30. Ratner, L., Haseltine, W., Patarca, R., Livak, K. J., Starcich, B., Josephs, S. F., Doran, E. R., Rafalski, J. A., Whitehorn, E. A., Baumeister, K., *et al.* (1985) *Nature (London)* **313,** 277–284.
31. Staley, J. & Kim, P. (1994) *Protein Sci.* **3,** 1822–1832.
32. Gross, E. & Witkop, B. (1961) *J. Am. Chem. Soc.* **83,** 1822–1832.
33. Mori, S., Abeygunawardana, C., Johnson, M. O. & van Zijl, P. C. (1995) *J. Magn. Reson. B* **108,** 94–98.
34. Pines, A., Gibby, M. G. & Waugh, J. S. (1973) *J. Chem. Phys.* **59,** 569–590.
35. Levitt, M. H., Suter, D. & Ernst, R. R. (1986) *J. Chem. Phys.* **84,** 4243–4255.
36. Wu, C. H., Ramamoorthy, A. & Opella, S. J. (1994) *J. Magn. Reson. A* **109,** 270–272.
37. Ramamoorthy, A., Wu, C. H. & Opella, S. J. (1995) *J. Magn. Reson. B* **107,** 88–90.
38. Teng, Q., Nicholson, L. K. & Cross, T. A. (1991) *J. Mol. Biol.* **218,** 607–619.
39. Opella, S. J., Stewart, P. L. & Valentine, K. G. (1987) *Q. Rev. Biophys.* **19,** 7–49.
40. Wu, C., Ramamoorthy, A., Gierasch, L. M. & Opella, S. J. (1995) *J. Am. Chem. Soc.* **117,** 6148–6149.
41. Kyte, J. & Doolittle, R. F. (1982) *J. Mol. Biol.* **157,** 105–132.
42. Cserzo, E., Wallin, E., Simon, I., von Heijne, G. & Elofsson, A. (1997) *Protein Eng.* **10,** 673–676.
43. Wray, V., Federau, T., Henklein, P., Klabunde, S., Kunert, O., Schomburg, D. & Schubert, U. (1995) *Int. J. Peptide Protein Res.* **45,** 35–43.
44. Federau, T., Schubert, U., Mossdorf, J., Henklein, P., Schomburg, D. & Wray, V. (1996) *Int. J. Peptide Protein Res.* **47,** 297–310.
45. Willbold, D., Hoffman, S. & Rosch, P. (1997) *Eur. J. Biochem.* **245,** 581–588.
46. Shon, K., Kim, Y., Colnago, L. A. & Opella, S. J. (1991) *Science* **252,** 1303–1305.
47. McDonnell, P. A., Shon, K., Kim, Y. & Opella, S. J. (1993) *J. Mol. Biol.* **233,** 447–463.
48. Marassi, F. M., Ma, C., Gesell, J. J. & Opella, S. J. (1999) *Appl. Magn. Reson.*, in press.
49. Mai, W., Hu, W., Wang, C. & Cross, T. A. (1993) *Protein Sci.* **2,** 532–542.
50. Bour, S., Geleziunas, R. & Wainberg, M. A. (1995) *Microbiol. Rev.* **59,** 63–93.
51. Miller, R. H. & Sarver, N. (1997) *Nat. Med.* **3,** 389–394.

BIOPHYSICS